Measuring mitochondrial Ca²⁺ efflux in isolated mitochondria and permeabilized cells

Julian DC Serna[1], Vitor de Miranda Ramos[1], João Victor Cabral-Costa[1], Eloisa A Vilas-Boas[1], Andressa G Amaral[2], Georgia Ohya[1], Camille C Caldeira da Silva[1], Alicia J Kowaltowski[1,*]

[1] Departamento de Bioquímica, Instituto de Química, Universidade de São Paulo, 05508-900, Brazil
[2] Departamento de Fisiologia, Instituto de Ciências Biomédicas, Universidade de São Paulo, 05509-900, Brazil

* Corresponding author: alicia@iq.usp.br

Abstract
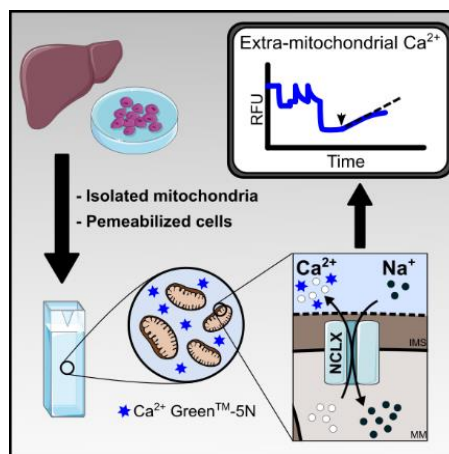
Mitochondrial Ca²⁺ efflux is essential for mitochondrial and cell Ca²⁺ homeostasis. Mitochondrial inner membrane Ca²⁺/H⁺ and Na⁺/Li⁺/Ca²⁺ (NCLX) exchangers are known today to be plastic transporters, with important roles in physiological responses and pathological states. Until now, however, no consensus protocols were available to measure mitochondrial Ca²⁺ efflux, and we find that some published protocols may induce mitochondrial permeability transition, underestimating the effects of these exchangers. In this work, we describe a method to measure Na⁺-sensitive and insensitive mitochondrial Ca²⁺ efflux activity in isolated mitochondria and permeabilized cells using the Ca²⁺ Green indicator and a fluorimeter. A checklist is provided to avoid artifacts as well as pinpoint adaptations necessary in specific experimental models.

Keywords – mitochondria; Ca²⁺ efflux; NCLX; mtPTP; liver

1. Introduction

Mitochondria are metabolic and signaling hubs, essential players in the life and death of eukaryotic cells (Spinelli, Haigis 2018; Giacomello et al 2020). Their ability to take up, store, and release calcium (Ca^{2+}) in a regulated manner helps shape spatiotemporal features of Ca^{2+} signaling events (Rizzuto et al 2012). Small and transient increases in Ca^{2+} within mitochondria physiologically regulate both oxidative phosphorylation and the production of oxidants but can also mediate organellar damage when in excessive amounts (Rossi et al 2019; Vercesi et al 2018; Vilas-Boas et al 2022). Mitochondrial Ca^{2+} uptake and release take place through independent pathways, and both activities are supported by protonmotive force (Giorgi et al 2018).

The MCU complex (MCUc) is the most active pathway for Ca^{2+} uptake (Figure 1) (Feno et al 2021). Conversely, three main pathways have been described for Ca^{2+} efflux (Giorgi et al 2018): (*1*) a Ca^{2+}/H^+ exchanger, the protein nature of which still lacks in consensus; (*2*) the sodium (Na^+) / lithium (Li^+) / Ca^{2+} exchanger (NCLX) that mediates Na^+-dependent Ca^{2+} release (Palty et al 2010); and (*3*) the mitochondrial permeability transition pore (mtPTP), which is a high conductance pathway that unselectively releases small molecules, including Ca^{2+}. mtPT is commonly induced by mitochondrial Ca^{2+} overload and oxidative imbalance (Figure 1) (Vercesi et al 2018).
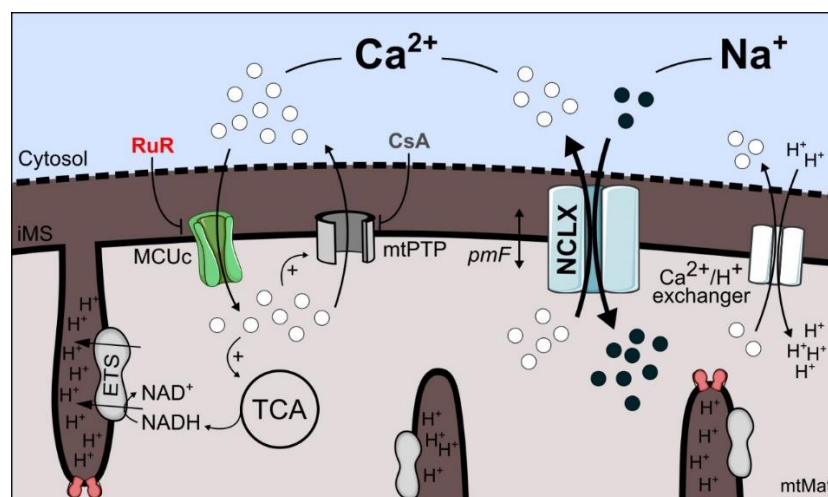
Figure 1. Mitochondrial inner membrane Ca²⁺ transport pathways. Ca^{2+} entry into the mitochondrial matrix (mtMat) from the intermembrane space (iMS) is mediated by the MCU complex (MCUc), a ruthenium red (RuR)-sensitive pathway. Ca^{2+} stimulates tricarboxylic acid cycle (TCA) dehydrogenases and inner mitochondrial membrane substrate transport. Ca^{2+} overload stimulates the formation of a high conductance pathway for Ca^{2+} efflux: the cyclosporin A (CsA)-inhibited mitochondrial permeability transition pore (mtPTP). Ca^{2+}/H^+ and $Na^+/Li^+/Ca^{2+}$ (NCLX) exchangers avoid matrix Ca^{2+} overload under physiological conditions. Both pathways depend on the proton electrochemical potential difference (*pmF*) generated by the electron transfer system (ETS).

Na^+-dependent mitochondrial Ca^{2+} efflux through NCLX has emerged as an important regulator of different cellular processes and may be a promising therapeutic target for diseases such as cancer (Pathak et al 2020) and Alzheimer´s (Jadiya et al 2019).

Thus, reliable protocols to test modulators of NCLX activity, as well as to investigate changes in its function, are needed. A comprehensive protocol would distinguish different efflux pathways and can be used for *in vivo* and *in vitro* studies.

Here, we briefly discuss the current pros and cons of available approaches to measure mitochondrial Ca^{2+} efflux and provide a step-by-step protocol to assess Ca^{2+} efflux rates in isolated mitochondria or permeabilized cells, focusing mainly on the activity of NCLX. We also discuss important experimental precautions that are essential to achieve reliable measurements.

1.1. Mitochondrial Ca^{2+} transport measurements in living cells

In experiments using living cells, Ca^{2+} concentrations ($[Ca^{2+}]$) are commonly assessed through imaging methods using either genetically encoded (Cameleons, Pericams, Aequorins, etc) or exogenous Ca^{2+} probes (such as acetoxymethyl esters of Fura 2 or Ca^{2+} Green™-5N), some of which can uncover Ca^{2+} signaling events at the subcellular level (Whitaker 2010; Grynkiewicz et al 1985; Minta et al 1989; Rudolf et al 2003). The free $[Ca^{2+}]$ in each cell compartment is the result of the balance between Ca^{2+} uptake, efflux, binding to chelators, and the formation of precipitates (Williams et al 2013).

Mitochondrial Ca^{2+} transport (uptake and efflux) is often studied by measuring cytoplasmic and matrix $[Ca^{2+}]$ during a signaling event. Although this approach does measure mitochondrial Ca^{2+} transport in a more physiological state, the complexity of the system does not always allow for accurate determinations of sources and mechanisms in which changes occur. Modulation of endoplasmic reticulum (ER) Ca^{2+} stores or the activity of plasma membrane Ca^{2+} transporters may alter cytoplasmic signals independently of mitochondrial ionic transport. Indeed, Ca^{2+} levels in the mitochondrial matrix are determined by several factors that involve mitochondrial Ca^{2+} uptake and extrusion properties, the proximity with the ER or plasma membrane, their ability to buffer or precipitate Ca^{2+}, and the matrix volume, among other factors (de Brito, Scorrano 2008; Nita et al 2012; Kuo et al 2019; Kowaltowski et al 2019). Notably, the formation of Ca^{2+} precipitates in the matrix makes it difficult to obtain true measurements of Ca^{2+} flux using these techniques, as it underestimates total uptake into the organelle. Other limitations in whole cell measurements involve difficulties with the use of pharmacological inhibitors, which often have off-target effects.

1.2. Assessment of mitochondrial Ca^{2+} transport in isolated mitochondrial preparations

A more reductionist approach to study Ca^{2+} transport using isolated mitochondrial samples solves several of the pitfalls mentioned above, although it does not, of course, uncover conditions *in situ*. On the other hand, the mitochondrial microenvironment can be tightly controlled with isolated preparations, including the availability/concentration of substrates, inhibitors, and ions (Na^+, $Ca^{2+,}$ and Li^+). Modulators such as ruthenium red (RuR – an MCU inhibitor) or CGP-37157 (CGP – an NCLX inhibitor) can dissect the effects of uptake and efflux pathways (Cox et al 1993).

Mitochondrial isolation from organs, tissues, or cell cultures relies on differential centrifugation and/or the use of density gradients (Gnaiger et al 2020; Gnaiger 2020). Mitochondrial isolation from cell cultures can be laborious and require large amounts of cells; in these models, permeabilized cell protocols are a more suitable option, as

discussed below. Isolation of mitochondria from organs is easier and in general gives good yields. While the reductionist approach using isolated mitochondria facilitates specific measurements and decreases artifacts, the physiological relevance of this approach is limited, and several caveats should be noted (Gnaiger et al 2020; Gnaiger 2020; Schmidt et al 2021), including that the mitochondrial population is biased, as swollen mitochondria may be lost during isolation, and the composition of the media does not truly reflect the cytoplasm. Several cytoplasmic components, such as proteins and metabolites, are essential regulators of mitochondrial function. In isolated brain mitochondria, for example, the absence of adenine nucleotides deeply impairs their ability to take up and store Ca^{2+}. In these cases, it is important to add ADP/ATP to the buffer (Kristian et al 2002; Amigo et al 2017). Finally, morphology and interactions with other cell components, such as membranes and cytoskeleton, are expectedly lost in isolated mitochondrial preparations.

Because of Ca^{2+} precipitation in the matrix, which leads to underestimation of total uptake when using intramitochondrial probes, extracellular Ca^{2+} probes can be more accurate choices to measure mitochondrial Ca^{2+} fluxes. Mitochondrial Ca^{2+} uptake assays to determine entry rates as well as uptake capacity are more frequently performed than efflux assays (examples can be seen in Amigo et al 2017; Serna et al 2020; Serna et al 2022). While quite straightforward, authors should note that the fluorescence of extramitochondrial probes can be influenced by media composition, making calibration under different conditions essential (Rudolf et al 2003).

Mitochondrial efflux assays are less commonly performed and have the added difficulty that distinguishing between the different pathways (Ca^{2+}/H^+, NCLX, or mtPTP) may be tricky. The main problems with measurements of Ca^{2+}/H^+ and NCLX activity are related to the masking effect of mtPT induction. As mitochondria must be loaded with Ca^{2+} to measure extrusion, permeability transition is often induced in at least a subset of the mitochondrial population, as we will show below. Since Ca^{2+} efflux through the exchangers is supported by protonmotive force, mtPT hampers the detection of the activity of both exchangers (Haworth et al 1980; Boyman et al 2013; Giorgi et al 2018).

1.3. Assessment of mitochondrial Ca²⁺ transport in permeabilized cells

Permeabilized cell models represent a midway option between living cell studies and isolated mitochondrial approaches (Fiskum et al 1980; Schmidt et al 2021). While they preserve cell architecture and the relationship between some organelles, they allow for direct control and access to the mitochondrial microenvironment, including precise Ca^{2+} uptake and release measurements using extramitochondrial Ca^{2+} sensors. Permeabilization is promoted by using substances such as digitonin, α-tomatin, or saponin to disrupt the integrity of the plasma membrane, preserving mitochondrial membranes, as well as mitochondrial morphology, interactions with other cell components, and function. This is achieved by titration of these detergents, and using the fact that mitochondria are poor in cholesterol (Fiskum et al 1980; Fiskum et al 2000; Vercesi et al 1991; Kuznetsov et al 2008; Saks et al 1998). Plasma membrane permeabilization establishes a continuity between the cytoplasm and the extracellular medium, allowing for experiments that modulate mitochondrial function directly, and avoiding any limitation imposed by the plasma membrane for substrate, inhibitor, or ion availability. Additional ion transport activities exerted by non-mitochondrial membranes

such as the ER are also excluded by permeabilization or using specific inhibitors as controls.

2. Mitochondrial Ca²⁺ efflux – isolated mitochondria

Isolated mitochondria may be obtained using many different protocols, and choices depend largely on the experimental model being studied. Here, we isolated mitochondria from the livers of 3 to 4-month-old male mice (C57BL/6NTac) and 6-month-old Sprague Dawley male rats (NTac: SD), as described previously (Tahara et al 2009, with modifications) and detailed below.

2.1. Liver mitochondrial isolation

Animal procedures were conducted in accordance with guidelines from the Ethical Committee for Animal Research (CEUA-IQ/USP 196/2021 and 109/2018). Animals were anaesthetized, euthanized, and had their livers immediately dissected. Mitochondria were isolated as follows:

1. Transfer the dissected liver (~1.5 g) to a beaker containing approximately 50 mL of ice-cold phosphate buffered saline (PBS) (Table 2). Keep all subsequent materials and solutions over ice.
2. Thoroughly mince the tissue into small fragments, using sharp scissors. Alternatively, a polytron grinder may be used to obtain a more homogeneous suspension and smaller organ fragments.
3. Wash repeatedly with PBS to remove excess contaminating blood.
4. Remove the PBS and add ice-cold isolation buffer to suspend the tissue fragments up to 2.5 % (m/V) (Table 3). For a whole mouse liver (or one quarter of a rat liver), this corresponds to ~60 mL.
5. Using an electric Potter-Elvehjem tissue grinder, homogenize the tissue (approximately five to six strokes, or until the tissue is clearly dissociated). Operate the Teflon pestle at 1 800 rpm.
6. Centrifugation #1 (remove cellular debris and blood): centrifuge at 900 g, 4 °C, for 4 min.
7. Transfer the supernatant to a new tube, discarding the pellet.
8. Centrifugation #2: re-centrifuge the supernatant at 900 g, 4 °C, for 4 min; discard the pellet.
9. Centrifugation #3 (pellet mitochondria): centrifuge the supernatant at 9000 g, 4 °C, for 5 min.
10. Discard the supernatant and resuspend the pellet in 60 mL of ice-cold isolation buffer (Table 3).
11. Centrifugation #4 (wash the pellet): centrifuge the suspension at 9000 g, 4 °C, for 5 min. Resuspend in 60 mL of ice-cold resuspension buffer (Table 4).
12. Centrifugation #5 (remove BSA from samples): centrifuge the resuspension at 9000 g, 4 °C, for 10 min.
13. For a whole mouse liver, resuspend the pellet in 300 µL ice-cold resuspension buffer (Table 4).
14. Maintain isolated mitochondria over ice to avoid degradation.
15. Measure protein concentrations using the Bradford method.

Note: Experiments were typically conducted with freshly isolated mitochondria soon after isolation and can be typically performed up to until 4 hours later, depending on sample run-down.

2.2. Defining ideal substrates by measuring Ca²⁺ retention capacity (CRC)

Before proceeding with the mitochondrial Ca²⁺ efflux assessment *per se*, it is of interest to determine the optimal conditions for the given experimental model. The ability to take up and store Ca²⁺ varies greatly depending on the organ or cells from which the mitochondria originated. Ions, proteins, and organic molecules in the experimental medium modulate the maximal amount of Ca²⁺ that can be taken up by mitochondria before overt mitochondrial mtPT induction. This upper limit of Ca²⁺ uptake ability is known as Ca²⁺ retention capacity (CRC). Mg²⁺ and adenine nucleotides (ATP, ADP, and AMP) may increase CRCs, while lipids and oxidants typically decrease CRCs (reviewed by Bonora et al 2022). In brain mitochondria, for example, adenine nucleotides are required in the medium to observe significant mitochondrial Ca²⁺ uptake (Amigo et al 2017). Our experimental medium also contains phosphate (P_i). Even though Pi can limit free Ca²⁺ concentration in the matrix, as Ca²⁺ precipitates are formed in its presence, we add it, as it is physiologically relevant and used in most experimental paradigms. The chosen energizing substrate(s) also deeply influence CRCs. In rat or mouse kidney mitochondria, for example, lower CRCs are observed when pyruvate and malate (which energize mitochondria mainly through Complex I) are employed as substrates, relative to succinate plus rotenone (which fuels electron transport mainly through Complex II) (Serna et al 2022).

Defining the optimal substrates involves measuring mitochondrial CRC under each condition. Ca²⁺ uptake assays are performed as shown in Figure 2 and described below.

2.2.1. Prepare the cuvette

1. Use a cuvette fluorimeter (we employed an F4500 Hitachi fluorimeter) with stirring and temperature control. Select an appropriate cuvette. For standard-sized 2 mL cuvettes, add 2 mM pyruvate plus 2 mM malate (or 2 mM succinate plus 1 μM rotenone), 15 μM EGTA, and 75 nM Calcium Green™-5N in 2 mL experimental buffer (Table 5).
   Note: the pH of substrates and EGTA needs to be adjusted to 7.2 using KOH when preparing the stock solutions.
2. Place the cuvette in the fluorimeter, with constant stirring, at 37 °C.
3. Wait a couple of minutes until the buffer temperature and composition are homogeneous.
4. Start measuring fluorescence at λ_{ex} = 506 nm and λ_{em} = 532 nm. Fluorimeter slits (or lamp voltage) should be adjusted to avoid saturation of the system.

2.2.2. Ca²⁺ loading traces to determine Ca²⁺ retention capacities

1. Add 0.5-1 mg of mitochondrial protein and wait for around 100 s for equilibration.
2. Perform sequential additions of 10 μM CaCl₂, waiting approximately 300 s between them or until the Ca²⁺ bolus is completely taken up by mitochondria. Usually, because of the EGTA present, a few CaCl₂ additions need to be made at the beginning of each trace before Ca²⁺ uptake is observed (marked by a

decrease in the Calcium Green™-5N fluorescence; true Ca^{2+} uptake exhibits an exponential-like decay shape, Figure 2).

3. Proceed with additions until a widespread mtPT in the mitochondrial population is reached, indicated by the increase in fluorescence in the absence of added Ca^{2+} boluses, or until fluorescence stabilizes after Ca^{2+} additions, with no further measurable mitochondrial uptake.
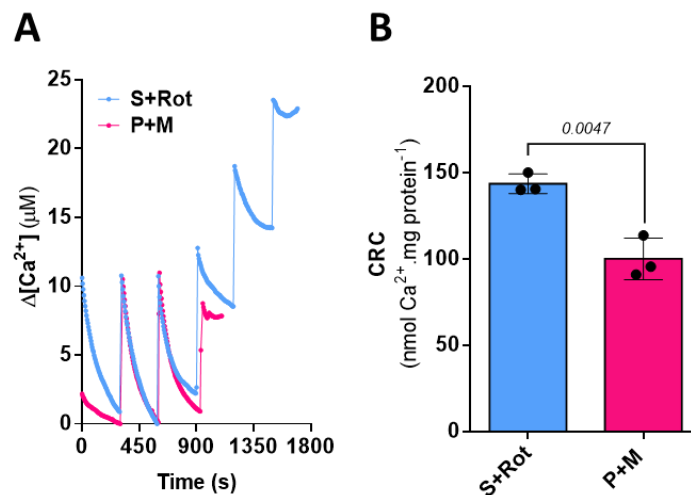

Figure 2. Ca^{2+} retention capacities in isolated mouse liver mitochondria: effect of different substrates. 500 μg liver mitochondria were incubated in 2 mL experimental buffer using either succinate plus rotenone (S+Rot) or pyruvate plus malate (P&M) as substrates. Extramitochondrial $[Ca^{2+}]$ were recorded over time using Calcium Green™-5N. (**A**) Typical Ca^{2+} uptake trace. Each peak in the trace results from the sequential addition of 10 μM $CaCl_2$ boluses in the media. The subsequent decrease in extramitochondrial $[Ca^{2+}]$ results from Ca^{2+} uptake into the matrix. When the ability to take up and store Ca^{2+} is surpassed, $[Ca^{2+}]$ in the media no longer decreases. (**B**) Quantified Ca^{2+} retention capacities (CRC), or the total amount of Ca^{2+} taken up per mg mitochondrial protein over the full loading trace, obtained from traces such as panel A. CRCs are higher when succinate (plus rotenone) is employed as the substrate. Distinct biological repetitions are indicated by individual data dots in panel B. Data were compared using an unpaired t-test and are presented as means ± SD.

2.3. Measuring mitochondrial Ca^{2+} efflux

Given the results seen in Figure 2, we chose succinate plus rotenone as the optimal energizing condition to measure Ca^{2+} efflux rates in mouse liver mitochondria. We can now proceed to conduct Ca^{2+} efflux measurements.

2.3.1. Choosing Ca^{2+} loads for efflux measurements: avoiding mtPTP opening

For obvious reasons, mitochondria must be loaded with Ca^{2+} to measure efflux rates, and different Ca^{2+} loads may generate different efflux rates. mtPTP opening, which is bolstered by higher Ca^{2+} loads, will interfere with exchanger activity measurements, as it eliminates or decreases protonmotive force. It should, thus, be avoided when measuring Ca^{2+}/H^+ exchanger and NCLX activities. Widespread mtPT induction is easily identifiable when measuring Ca^{2+} fluxes, as it leads to overt Ca^{2+} release, but we find it can often be overlooked when affecting a subset of the mitochondrial population, as exemplified by the

results in Figure 3: Mitochondria were loaded with three different amounts of Ca²⁺, and subsequent extrusion rates were measured in the absence or presence of mtPTP inhibitor cyclosporin A (CsA). We find that CsA-insensitive Ca²⁺ efflux (Ca²⁺/H⁺ efflux, in this instance, since Na⁺ was not added) is similar under all conditions tested. However, total efflux rates increase with increasing Ca²⁺ loads due to a CsA-sensitive activity, which indicates that the mtPTP was responsible. These results demonstrate that using higher Ca²⁺ loads promotes mtPTP opening even when the CRC has not been exceeded. Indeed, electron microscopy data support the heterogeneity of mtPTP induction (Beatrice et al 1982).
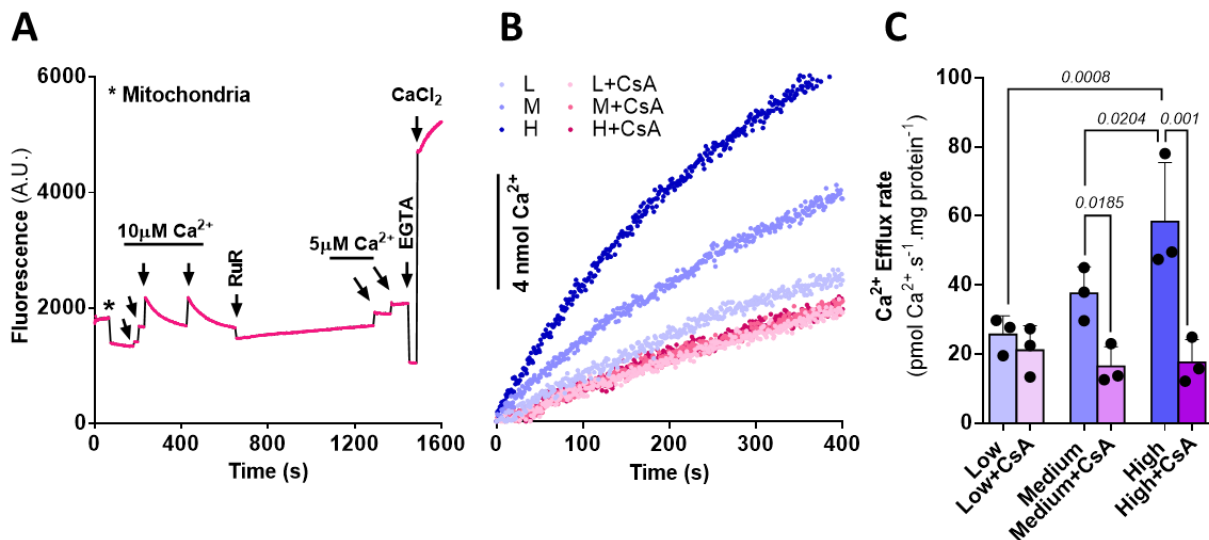

Figure 3. Permeability transition in mitochondrial subpopulations affects Ca²⁺ efflux measurements. 500 µg liver mitochondria were incubated in 2 mL experimental buffer with 2 mM succinate plus 1 µM rotenone. Extramitochondrial Ca²⁺ concentrations were recorded using Calcium Green™-5N. (**A**) Representative plot for the full Ca²⁺ efflux assay, following Calcium Green fluorescence over time. Mitochondria were added (*) and allowed to equilibrate. The first two 10 µM CaCl₂ additions did not result in ion uptake as the chelator EGTA was present (discussed above). The gradual decrease in fluorescence observed after the third and fourth CaCl₂ additions is due to mitochondrial Ca²⁺ uptake. After the 40 nmol Ca²⁺ load, ruthenium red (RuR) was added, resulting in a small immediate fluorescence quenching. The slow increase in fluorescence that follows is due to mitochondrial Ca²⁺ efflux. After several minutes recording this efflux, two sequential additions of 5 µM CaCl₂ were performed for calibration purposes. Along with this, minimal and maximal fluorescence values were determined by the addition of 1.5 mM EGTA and 10 mM CaCl₂, respectively. (**B**) Representative Ca²⁺ efflux traces. Initially, mitochondria were loaded either with low (L - 20 nmol), medium (M - 40 nmol) or high (H - 60 nmol) amounts of Ca²⁺, in the presence or absence of 5 µM cyclosporin A (CsA). To measure mitochondrial Ca²⁺ efflux, ruthenium red (RuR) was added, and extrusion was followed over time. (**C**) Initial Ca²⁺ efflux rates were determined as the slope of the linear portion of the efflux trace just after RuR addition. Distinct biological repetitions are indicated by individual data dots in panel C. Data were compared using repeated measures one-way ANOVA with Tukey's multiple comparisons test and are presented as means ± SD.

BEC

2.3.2. Measuring mtPT- and Na⁺-independent mitochondrial Ca²⁺ efflux

We established that the CsA-sensitive efflux rate under our conditions was not significant when 40 nmol Ca^{2+}/mg mitochondrial protein were employed as a calcium load, and used this condition to study exchanger-dependent Ca^{2+} efflux, as follows:

1. Add 0.5-1 mg of mitochondria to a fluorimeter cuvette and media containing Calcium Green™-5N, as described in uptake experiments, above. Wait around 100 s for equilibration.

   Note: experimental modulators of mitochondrial activity, such as CsA, CGP, or ATP, should be added before mitochondria. If a low enough Ca^{2+} load to avoid mtPTP opening cannot be achieved, CsA may be used in all traces.

2. Add 40 nmol $CaCl_2$/mg mitochondrial protein and wait for fluorescence to stabilize after Ca^{2+} is taken up.

   Note: sequential additions may be needed to overcome EGTA chelation. Assessing the activity of Ca^{2+} exchangers requires Ca^{2+} load optimization to avoid mtPTP opening (see critical point above).

3. Add 0.5-2.5 μM RuR (or another MCU inhibitor) to inhibit mitochondrial Ca^{2+} uptake.

   Note: final RuR concentrations should be titrated for each mitochondrial amount employed. Wingrove and Gunter (1986) observed inhibition of Na⁺-stimulated Ca^{2+} efflux in liver mitochondria with RuR above 10 nmol/mg protein. In liver, kidney, and heart mitochondria, we find 0.5-2.5 μM RuR works well.

4. Record Ca^{2+} efflux during at least 400 s. We will refer to the Na⁺-independent mitochondrial Ca^{2+} efflux (or non-stimulated Ca^{2+} efflux) as basal efflux from here onward.

2.3.3. Measuring Na⁺-dependent mitochondrial Ca²⁺ efflux

The protocol to assess Na⁺(or Li⁺)-stimulated Ca^{2+} efflux is essentially the same as that to measure basal Ca^{2+} efflux, but with added Na⁺:

1. Repeat steps 1-3 above.
2. After Ca^{2+} loading and inhibition of the MCU with RuR, allow the system to equilibrate for 100-200 s.
3. Add 20 mM NaCl (or LiCl) to induce a Na⁺(Li⁺)-dependent Ca^{2+} efflux. Record fluorescence changes for at least 400 s.

   Note: Ca^{2+} efflux rates must be calculated and compared using the same initial and final time points: matrix Ca^{2+} concentrations decrease over time, and efflux rates do too.

4. To estimate NCLX-dependent efflux, subtract the basal efflux rate from the with Na⁺ stimulation.

Figure 4 shows an example in which Ca^{2+} efflux rates were measured in isolated mouse liver mitochondria. We observed significant and similar Na⁺ and Li⁺ stimulation of Ca^{2+} efflux under these conditions, indicating the presence of NCLX activity corresponding to more than half of the total extrusion activity in these mitochondria. Our results contrast with those of others, who were unable to observe Na⁺-stimulated efflux in liver mitochondria (Rysted et al 2021), possibly due to mtPTP induction, given a high Ca^{2+} load was employed. Indeed, Haworth et al (1980) reported similar Na⁺-stimulated efflux values to those we obtained, and Wingrove and Gunter (1986) also observed Na⁺-stimulated efflux in liver mitochondria.
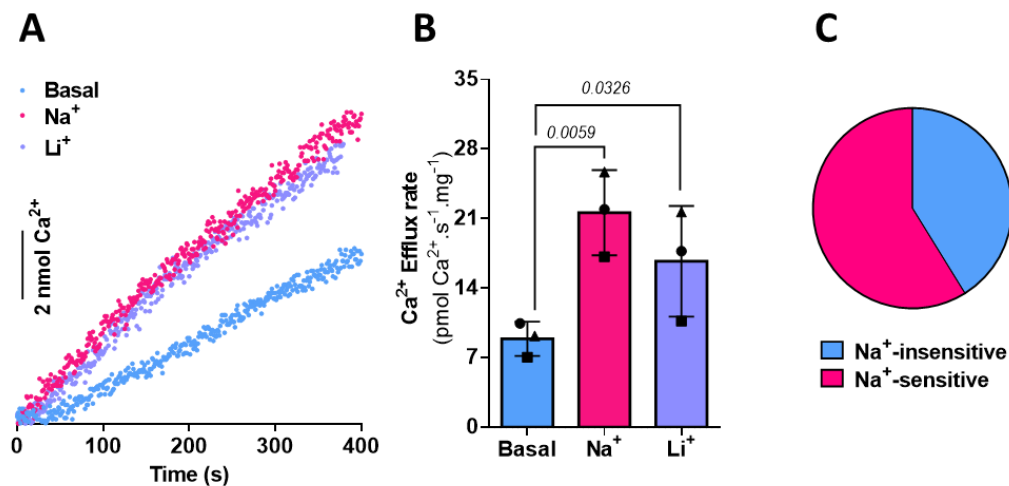
Figure 4. Ca²⁺ efflux in mouse liver mitochondria. 1 mg liver mitochondria was incubated in 2 mL experimental buffer with 2 mM succinate plus 1 μM rotenone. Extramitochondrial Ca²⁺ was recorded using Calcium Green™-5N. (**A**) Typical Ca²⁺ extrusion traces. Mitochondria were loaded with 40 nmol Ca²⁺, as shown in Figure 3, and then treated with 1.25 μM RuR. Ca²⁺ efflux was measured under basal conditions (non-stimulated) or stimulated with 20 mM Na⁺ or Li⁺, as indicated. (**B**) Ca²⁺ efflux rates were determined from the slope just after Na⁺ or Li⁺ additions. (**C**) Relative contribution of Na⁺-sensitive and Na⁺-insensitive Ca²⁺ efflux pathways. Data were compared using repeated measures one-way ANOVA with Tukey's multiple comparisons test and are presented as means ± SD. Distinct biological repetitions are indicated by individual data dots in panel B.

We also measured mitochondrial Ca²⁺ efflux rates in rat liver mitochondria, Figure 5. We observed similar Na⁺-dependent and independent effluxes to those measured by us in mouse liver mitochondria. To further characterize if this Na⁺-dependent efflux activity is due to NCLX, we measured efflux rates in the presence of Li⁺, K⁺, and Na⁺ plus CGP-37157. Li⁺ stimulates Ca²⁺ efflux, but to a lesser extent than Na⁺. K⁺ did not enhance Ca²⁺ efflux, as expected (Haworth et al 1980). CGP-37157, a widely recognized NCLX selective inhibitor (Cox et al 1993), completely abolished Na⁺-stimulated Ca²⁺ efflux. Overall, our results support the existence of NCLX in mouse and rat livers.

2.3.4. Calibration: transforming Calcium Green fluorescence to [Ca²⁺]

Fluorescence changes of the Calcium Green™-5N probe should be transformed into [Ca²⁺] by calibrating. We find that the addition of some mitochondrial modulators and ions alters probe response to changes in [Ca²⁺], so calibrations should be conducted separately for each experimental condition, as follows (see a sample trace in Figure 3A):

1. At the end of each experimental trace, make at least two consecutive additions of 5 μM $CaCl_2$ to the experimental media while recording Calcium Green fluorescence.
2. Add 1.5 mM EGTA (or more, if necessary) to achieve minimal Calcium Green fluorescence (F_{min}).
3. Add 10 mM $CaCl_2$ (or more, if necessary) to reach maximal Calcium Green fluorescence (F_{max}).

4. K_d calculation: The K_d is empirically determined as the value in which the change in fluorescence (ΔF) before and after Ca^{2+} additions fits the 5 µM Ca^{2+} increase. This process is made by iteration, as follows:

Convert all fluorescence values to $[Ca^{2+}]$ according to the equation $[Ca^{2+}] = K_d \cdot (F - F_{min})/(F_{max} - F)$ by using a pre-determined K_d value (e.g. 50 µM).
Calculate the $\Delta[Ca^{2+}]$ from before and after the 5 µM $CaCl_2$ additions.
Decrease or increase the K_d value in the formula until the $\Delta[Ca^{2+}]$ value is equal to 5 µM (iteration).

5. Calculate calcium concentrations for the experimental traces using the K_d value obtained and the formula: $[Ca^{2+}] = K_d \cdot (F - F_{min})/(F_{max} - F)$.
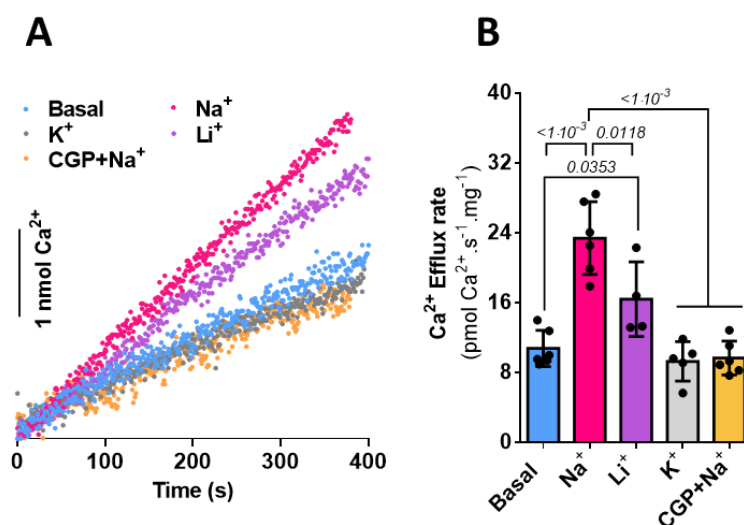

Figure 5. Ca^{2+} efflux in rat liver mitochondria. 500 µg liver mitochondria were incubated in 2 mL experimental buffer with 2 mM pyruvate plus 2 mM glutamate. Extramitochondrial Ca^{2+} was recorded using Calcium Green™-5N. (**A**) Typical Ca^{2+} extrusion traces. Mitochondria were loaded with 20 nmol Ca^{2+}, as shown in Figure 3, and then treated with 1.25 µM RuR. Ca^{2+} efflux was measured under basal conditions (non-stimulated) or stimulated with 20 mM Na^+, 20 mM K^+, 20 mM Li^+, or 20 mM Na^+ in the presence of 5 µM CGP-37157, as indicated. (**B**) Ca^{2+} efflux rates were determined from the slope just after Na^+, Li^+, or K^+ additions. Distinct biological repetitions are indicated by individual data dots in panel B. Data were compared using one-way ANOVA with Tukey's multiple comparisons test; data are presented as means ± SD.

3. Mitochondrial Ca^{2+} efflux – permeabilized cells

Permeabilized cells allow for assessments using protocols similar to those used for isolated mitochondria, once optimal permeabilization conditions are established. We demonstrate here using human hepatoma PLC/PRF/5 cells.

3.1. Digitonin titration for optimal permeabilization

We employed digitonin to selectively permeabilize cell membranes without disturbing mitochondrial integrity. Optimal digitonin concentrations were determined using an O2k high-resolution oxygraph (Oroboros Instruments, Austria). The titration assay relies on the low permeability of the plasmalemma to succinate, a restraint removed when the membrane is permeabilized, resulting in increased mitochondrial oxygen

consumption rates in the presence of rotenone. ADP is commonly added to increase respiration and titration sensitivity. A detailed digitonin titration protocol is:

3.1.1. Prepare the cell suspension
1. Plate cells to obtain $> 1 \cdot 10^6$ cells at the desired confluence (e.g., a 100 mm culture dish per trace).
2. Wash cells with warm PBS.
3. Add 2 mL of trypsin-EDTA solution and incubate at 37 °C for 3-5 min (depending on cell type).
4. Inhibit trypsin with 4 mL culture media.
5. Collect cells and centrifuge at 200 g for 5 min.
6. Wash cells: resuspend in 4 mL experimental buffer supplemented with 1 mM EGTA.
7. Mix gently with a widened (cut) 1000 µL pipette tip to disaggregate any cell clumps.
8. Centrifuge the cell suspension at 200 g for 5 min.
9. Resuspend cells in 500 µL experimental buffer with 1 mM EGTA. Dilute the cell suspension (if required) and count viable cells.
    Note: when cells have a strong tendency to form clumps, dilute the cells with PBS supplemented with EGTA and EDTA before counting.

3.1.2. Titrating digitonin concentrations
1. Add 2 mM succinate, 1 µM rotenone, and 1 mM ADP to experimental buffer in an O2k-chamber.
2. Add the cell suspension for a final cell concentration of $0.5 \cdot 10^6$ x·mL⁻¹ in 2 mL experimental buffer (supplemented 1 mM EGTA).
3. Make sequential 0.5 % digitonin additions (aim for incremental additions of 0.5–1 µL) and observe oxygen consumption increases. When digitonin amounts are excessive, oxygen consumption rates will gradually decrease (Figure 6).
    Note: allow time for oxygen flux stabilization. Initial digitonin additions are more time-demanding (usually between 2–6 min).
4. Optimal digitonin concentrations will be those that induce highest mitochondrial respiration.

3.1.3. Mitochondrial outer membrane integrity assay

To validate cell permeabilization quality, a control for mitochondrial outer membrane integrity can be performed. Excessive amounts of digitonin lead to outer membrane permeabilization and subsequent cytochrome c release. Under these conditions, oxygen consumption rates are lower. The assay can be conducted as follows:

1. Add 2 mM succinate and 1 µM rotenone to experimental buffer in an O2k-chamber, plus the chosen digitonin concentration.
2. Add the cell suspension at a final cell concentration of $0.5 \cdot 10^6$ x·mL⁻¹.
3. Measure oxygen consumption in P: add 1 mM ADP.
4. Measure oxygen consumption in P + cytochrome c: add 10 µM cytochrome c.
5. Measure oxygen consumption in L (LEAK respiration): add 1 µM oligomycin.
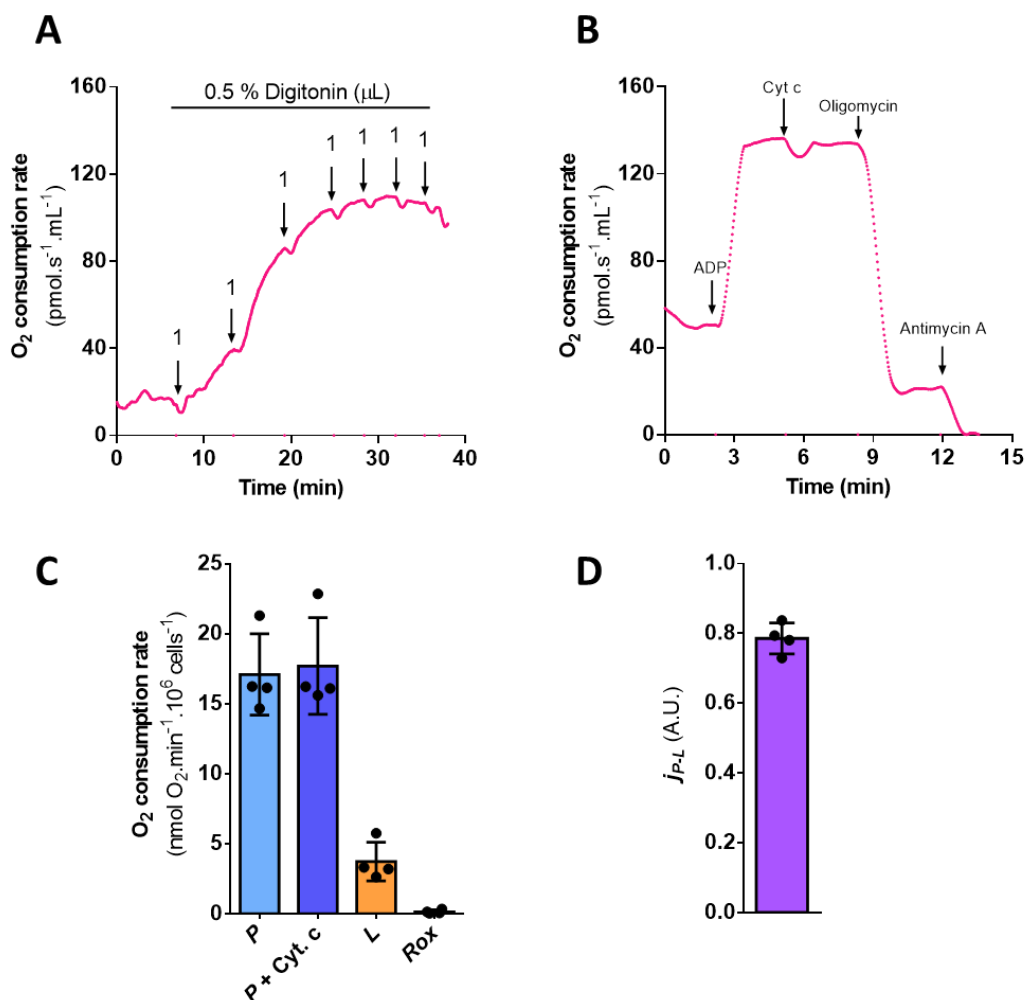6. Measure Rox (residual oxygen consumption): add 1 µM antimycin A.

Figure 6. Optimization of cell permeabilization by digitonin. $1 \cdot 10^6$ PLC/PRF/5 cells were incubated in 2 mL experimental buffer the presence of 2 mM succinate and 1 µM rotenone. Oxygen consumption rates were measured with an Oroboros O2k. (**A**) Titration: sequential additions of 1 µL of 0.5% digitonin were made until respiratory inhibition was observed; 1 mM ADP was present from the beginning. (**B**) Representative trace for outer mitochondrial membrane integrity assessment using cytochrome *c* (cyt c) and $6.25 \cdot 10^{-3}$ % digitonin. 1 mM ADP, 10 µM cytochrome *c*, 1 µM oligomycin, and 1 µM antimycin A were added where indicated. (**C**) Quantifications for traces such as in Panel B; OXPHOS capacity (*P*), LEAK respiration (*L*) and Residual oxygen consumption (*Rox*). (**D**) *P-L* control efficiency (j_{P-L}) was determined as 1-(*L/P*). Distinct biological repetitions are indicated by individual data dots in panels C and D.

Exogenous cytochrome *c* addition in the media recovers normal electron transfer activity if the outer membrane is ruptured. If cells have been properly permeabilized, no differences should be detected between respiratory rates in *P* (OXPHOS capacity: saturating ADP and P_i) and *P* plus cytochrome *c*. As shown in Figure 6, the chosen digitonin concentration does not induce outer mitochondrial membrane disruption.

3.2. Define ideal substrates by measuring CRC

Follow the experiments described in Section 2.2 to determine ideal substrates to use with your cell type.

3.3. Measuring mitochondrial Ca²⁺ efflux and assessing NCLX activity

Mitochondrial Ca²⁺ efflux assessment in permeabilized suspended cells follows similar protocols to those described for isolated mitochondria:

3.3.1. Prepare the cuvette
1. Add the chosen substrates and 20–40 µM EGTA in experimental buffer (Table 5) plus 75 nM Calcium Green™-5N and the optimal digitonin concentration, as defined above.
   Note: modulators of mitochondrial function, such as CsA, ATP, or CGP, should be added before the cells.
   Note: EGTA concentrations are titrated in preliminary experiments, as follows: first, permeabilize cells in experimental medium supplemented with a small amount of EGTA, i.e. 10 µM EGTA. If Ca²⁺ uptake is observed (marked by an exponential decay shaped decrease in fluorescence), increase EGTA concentrations until uptake is no longer present. Repeat the experiment with the concentration determined previously and verify if mitochondrial Ca²⁺ uptake is not observed since the beginning of the trace.
2. Place the cuvette in the fluorimeter, with constant stirring, at 37 °C.
3. Wait a couple of minutes until the buffer temperature and composition is homogeneous.
4. Start measuring fluorescence at λ_{ex} = 506 nm and λ_{em} = 532 nm. Fluorimeter slits (or lamp voltage) should be adjusted to avoid saturation of the system.

3.3.2. Ca²⁺ loading
1. Add $1·10^6$ cells and wait around 100 s for equilibration.
2. Add 10 µM (or 5 µM) CaCl₂ until cells have been loaded with 20–30 nmol Ca²⁺/ $1·10^6$ cells. Usually, a few CaCl₂ additions are necessary before Ca²⁺ uptake is observed.
   Note: As discussed previously for isolated mitochondrial preparations, low Ca²⁺ loads are necessary to avoid mtPTP opening.
3. Add 1.25 µM RuR to inhibit mitochondrial Ca²⁺ uptake.

3.3.3. Mitochondrial Ca²⁺ efflux
3.1 Record Ca²⁺ efflux during at least 700 s to determine basal efflux rates (non-stimulated Ca²⁺ efflux).
3.2 Add 20 mM NaCl or LiCl to induce a Na⁺(Li⁺)-dependent Ca²⁺ efflux, as shown in Figure 7. NCLX activity can be tested measuring Na⁺-dependent Ca²⁺ efflux in the presence of 5 µM CGP-37157.
   Note: Ca²⁺ efflux rates must be calculated at equal time points, as discussed for isolated mitochondria, so parallel control experiments with/without Na⁺ or Li⁺ should be conducted.
3.3 Calibrate traces as described above.

3.3.4. Calibration: transforming Ca²⁺-Green fluorescence into [Ca²⁺]

Fluorescence traces should be transformed into [Ca²⁺] measurements, as described in Section 2.3. Experimental and calibration steps can be combined in the same trace, as shown in Figure 3A.
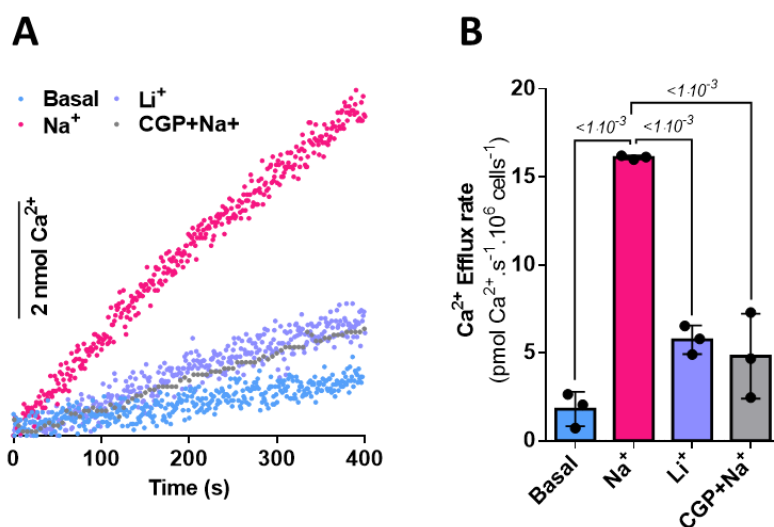
BEC

Figure 7. Mitochondrial Ca^{2+} efflux in permeabilized PLC cells. $1·10^6$ PLC/PRF/5 cells were incubated in 2 mL buffer in the presence of 2 mM succinate, 1 μM rotenone, and $6.25·10^{-3}$ % digitonin. Ca^{2+} efflux was recorded following Calcium Green^{TM}-5N fluorescence at 37 °C. (**A**) Representative Ca^{2+} efflux trace. Mitochondria were loaded with 20 nmol Ca^{2+} and then treated with 1.25 μM RuR. Ca^{2+} efflux was measured under either basal conditions or stimulated with 20 mM Na$^+$, Li$^+$, or 20 mM Na$^+$ in the presence of 5 μM CGP-37157. (**B**) Ca^{2+} efflux rates were quantified from the slope of the linear portion of the efflux trace just after Na$^+$ or Li$^+$ additions (or 200 s after RuR addition in the basal condition group). Distinct biological repetitions are indicated by individual data dots in panel B. Data were compared using repeated measures one-way ANOVA with Tukey's multiple comparisons test and are presented as means ± SD.
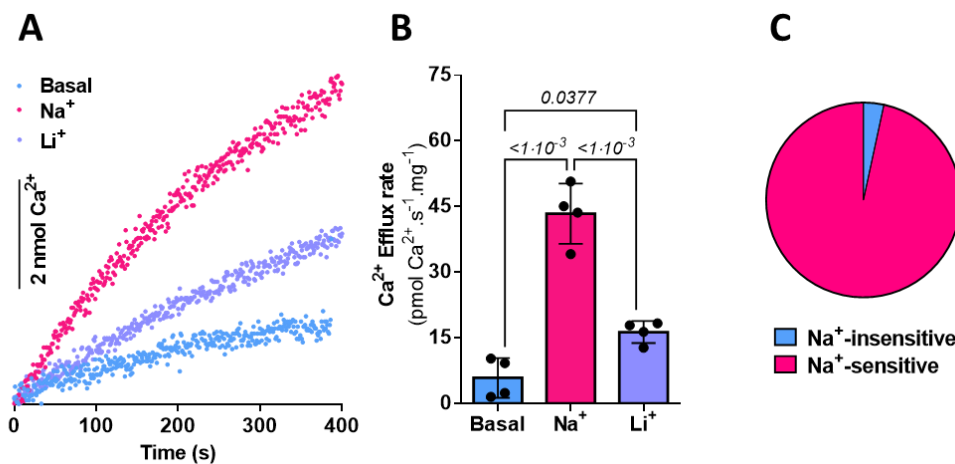

Figure 8. Ca^{2+} efflux in rat heart mitochondria. 500 μg of heart mitochondria were incubated in 2 mL experimental buffer in the presence of 2 mM succinate plus 1 μM rotenone. Extramitochondrial Ca^{2+} concentrations were recorded over time using Calcium Green^{TM}-5N. (**A**) Typical Ca^{2+} release traces. Mitochondria were loaded with 20 nmol Ca^{2+} and then treated with 1.25 μM RuR. Ca^{2+} efflux was measured under basal conditions or stimulated with 20 mM Na$^+$ or Li$^+$. (**B**) Ca^{2+} efflux rates were determined as the slope of the linear portion of the efflux trace just after Na$^+$ or Li$^+$ addition (or 200 s after RuR addition in the basal condition group). (**C**) Relative contribution of Na$^+$-sensitive and Na$^+$-insensitive Ca^{2+} efflux pathways. Distinct biological repetitions are indicated by individual data dots in panel B. Data were compared using repeated measures one-way ANOVA with Tukey's multiple comparisons test and are presented as means ± SD.

4. Protocol Validation and Reproducibility

To demonstrate the robustness of our protocols, we validated their applicability in two additional models: rat heart mitochondria and the INS-1E insulinoma cell line.

4.1. Isolated heart mitochondria

Rat heart mitochondria were isolated using a protocol that includes both subsarcolemmal and intermyofibrillar mitochondria (Gostimskaya, Galkim 2010; Serna et al 2020). We then measured Ca²⁺ efflux rates as described above for liver mitochondria; results are presented in Figure 8. We find that the protocol is also appropriate for Ca²⁺ efflux measurements in heart mitochondria, and also confirm data from previous work (Rysted et al 2021) demonstrating that the Na⁺-sensitive pathway is predominant in heart, but that it is less stimulated by Li⁺.
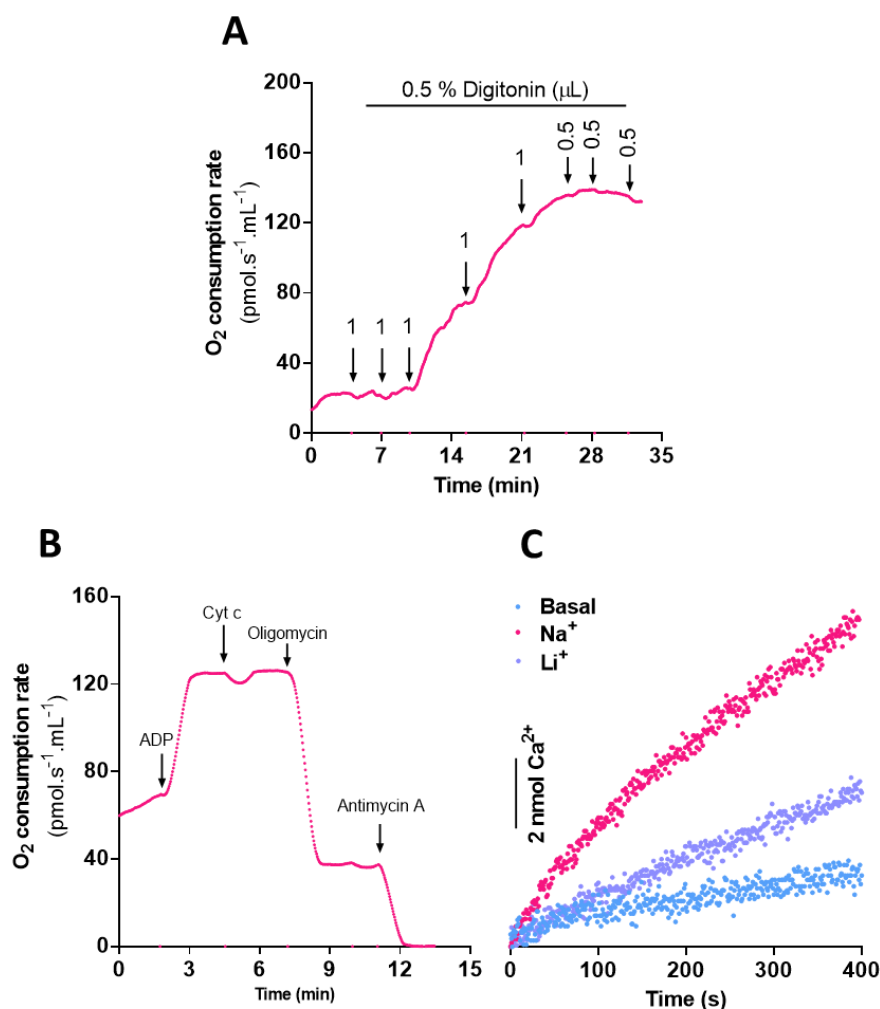

Figure 9. Digitonin titration and Ca²⁺ efflux measurements in permeabilized INS-1E cells. 2.5·10⁶ INS-1E cells were incubated in 2 mL experimental buffer the presence of 2 mM succinate plus 1 µM rotenone. Oxygen consumption rates were measured with an O2k. (**A**) Titration: 1 mM ADP was added and sequential additions of 0.5 or 1 µL of 0.5 % digitonin were made where indicated. (**B**) Representative trace for outer mitochondrial membrane integrity assessment using cytochrome *c* (cyt *c*). Mitochondrial activity was modulated by the sequential addition of 1 mM ADP, 10 µM cyt *c*, 1 µM oligomycin, and 5 µM antimycin A. (**C**) Representative Ca²⁺ efflux trace. Mitochondria were loaded with 20 nmol Ca²⁺ and then treated with 1.25 µM RuR. Ca²⁺ efflux was measured under basal conditions (non-stimulated) or stimulated with 20 mM Na⁺ or Li⁺.

4.2. Digitonin-permeabilized INS-1E cells

INS-1E cells were trypsinized, collected, and counted as we described for PLC/PRF/5 cells. Digitonin was titrated and outer mitochondrial integrity controls were performed (Figure 9 A,B). Ca^{2+} efflux was assessed as in Section 3.3 (Figure 9C). As described for PLC cells, Na^+ and Li^+ are able to stimulate Ca^{2+} efflux, demonstrating that the described protocol is adaptable to other cell types.

5. Troubleshooting

Table 1. Troubleshooting

Problem	Possible reason	Solution
High basal (Na^+-independent) Ca^{2+} efflux rates, or low Na^+-sensitive Ca^{2+} efflux rates.	Mitochondrial permeability transition is being induced.	Decrease mitochondrial Ca^{2+} load or add cyclosporin A.
Ca^{2+} uptake/efflux trace is noisy	Mitochondrial clumps are present in isolated mitochondrial samples.	Gently disaggregate mitochondrial pellets using a brush with soft bristles.
	Cells are not properly dissociated, forming clumps. Cell culture trypsinization is insufficient.	Optimize trypsinization protocol for each cell type.
	Dead cells release DNA, promoting clump formation.	Decrease trypsinization time (or trypsin amount).
Cytochrome c stimulates P oxygen consumption rates	Mitochondrial outer membrane permeabilization and cytochrome c release leading to electron transfer impairment.	Decrease digitonin concentrations in the experimental medium.
Abundant cell clumps when counting	Cell-cell interactions are preserved after sample preparation; these interactions are induced by Ca^{2+} and Mg^{2+}.	Dilute cell stocks in PBS supplemented with EDTA before counting.

6. Conclusion

We describe a method to measure Ca^{2+} efflux in isolated mitochondria and permeabilized cells, as indicated in the workflow in Figure 10. Our approach allows us to dissect between Na^+-sensitive and insensitive Ca^{2+} efflux. We demonstrate that a vital point in obtaining consistent and reliable Ca^{2+} extrusion activity measurements through mitochondrial exchangers is to avoid mtPTP opening by either using low Ca^{2+} loads or adding cyclosporin A to all traces. In the absence of this step, at least part of the activity of NCLX and Ca^{2+}/H^+ exchange may be masked by mtPTP-promoted permeabilization. Using this method, we were able to demonstrate NCLX activity in isolated mouse and rat liver mitochondria, as well as permeabilized liver hepatoma PLC/PRF/5 cells. Additionally, we validated our method in isolated rat heart mitochondria, as well as the insulinoma INS-1E cell line.
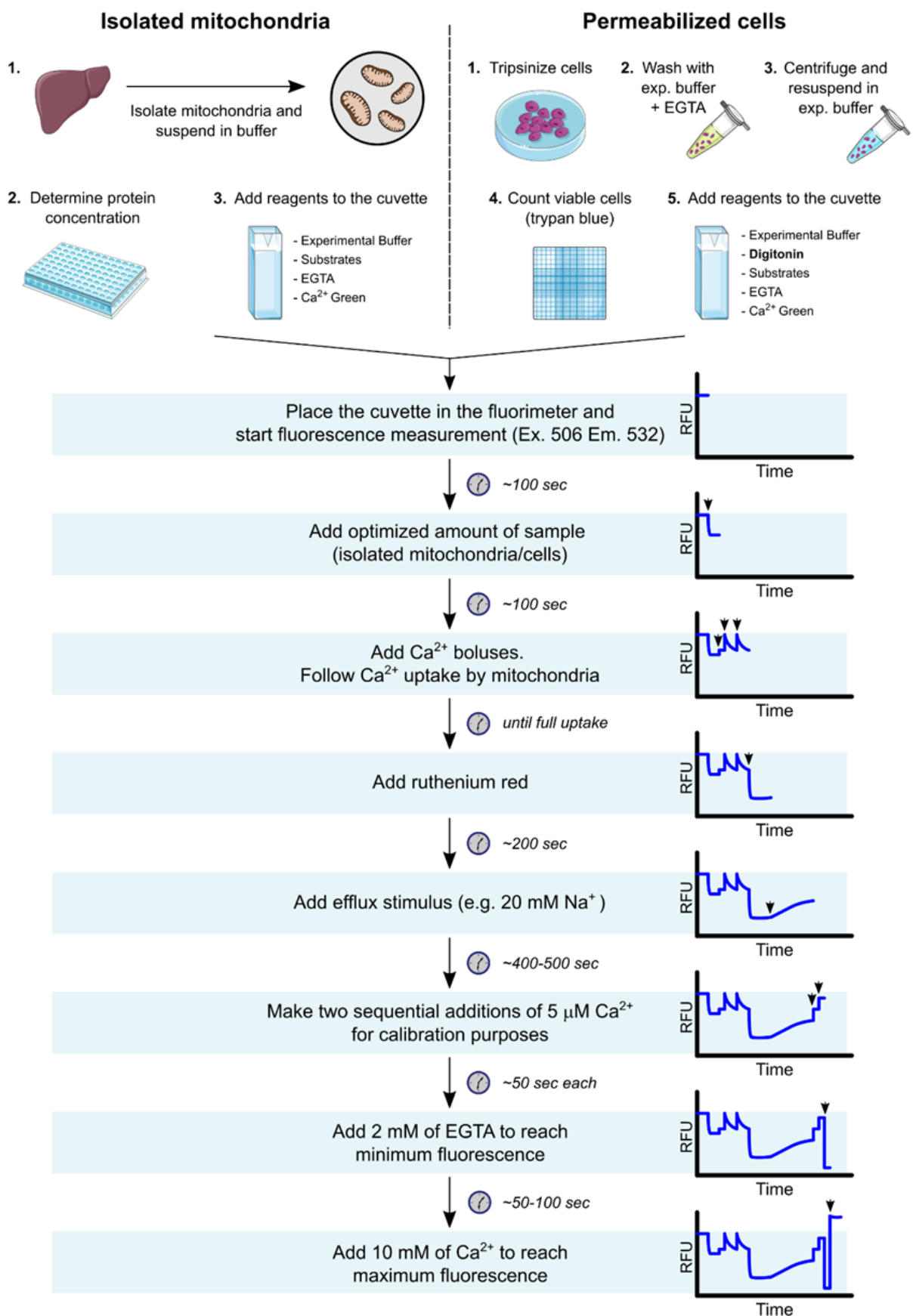
Figure 10. Schematic workflow for mitochondrial Ca²⁺ efflux measurements.

BEC

7. Media composition tables

Table 2. Phosphate buffered saline (pH = 7.4, adjusted with NaOH)

Reagent	Final concentration	Amount
NaCl	1.37 M	80.01 g
KCl	27 mM	2.01 g
Na_2HPO_4	100 mM	14.2 g
KH_2PO_4	18 mM	2.45 g
EDTA	10 mM	3.8 g
milliQ H₂O	-	**adjust to 1 L**

Table 3. Liver isolation buffer (pH = 7.2, adjusted with KOH)

Reagent	Final concentration	Amount
Sucrose	250 mM	85.57 g
Hepes	10 mM	2.38 g
EGTA	1 mM	380 mg
EDTA	1 mM	380 mg
BSA (fatty-acid free)	1 mg/mL	1 g
milliQ H₂O	-	**adjust to 1 L**

Note: To avoid formation of bubbles or clumps when diluting BSA, add the powder over the solution and leave still for a while. Adjust pH only with KOH and HCl. Store at 4 ℃ for up to a month.

Table 4. Resuspension buffer (pH = 7.2, adjusted with KOH)

Reagent	Final concentration	Amount
Sucrose	300 mM	20.54 g
Hepes	10 mM	476 mg
EGTA	2 mM	152 mg
milliQ H₂O	-	**adjust to 200 mL**

Store at 4 ℃ for up to a month.

Table 5. Experimental buffer (pH = 7.2, adjusted with KOH)

Reagent	Final concentration	Amount
Sucrose	125 mM	21.39 g
KCl	65 mM	2.42 g
Hepes	10 mM	1.19 g
$MgCl_2$	2 mM	95 mg
KH_2PO_4	2 mM	136 mg
BSA (fatty acid-free)	0.1 mg/mL	50 mg
milliQ H₂O	-	**adjust to 500 mL**

To avoid formation of bubbles or clumps when diluting BSA, add the powder over the solution and leave it without stirring for a while. Store at 4 ℃ for up to a month. Adjust pH only with KOH and HCl.

Abbreviations

pmF	protonmotive force	ETS	electron transfer system
Rox	residual oxygen consumption	mtPTP	mitochondrial permeability
BSA	bovine serum albumin		transition pore
CGP	CGP-37157	NCLX	$Na^+/Li^+/Ca^{2+}$ exchanger
CRC	calcium retention capacity	*j_{P-L}*	*P-L* control efficiency
CsA	Cyclosporin A	RuR	Ruthenium Red
Cyt c	cytochrome *c*	*P*	OXPHOS capacity
		L	LEAK respiration

Acknowledgements

References

Amigo I, Menezes-Filho SL, Luévano-Martínez LA, Chausse B, Kowaltowski AJ (2017) Caloric restriction increases brain mitochondrial calcium retention capacity and protects against excitotoxicity. https://doi.org/10.1111/acel.12527

Beatrice MC, Stiers DL, Pfeiffer DR (1982) Increased permeability of mitochondria during Ca²⁺ release induced by t-butyl hydroperoxide or oxalacetate. The effect of ruthenium red. https://doi.org/10.1016/S0021-9258(18)34551-4

Bonora M, Giorgi C, Pinton P (2022) Molecular mechanisms and consequences of mitochondrial permeability transition. https://doi.org/10.1038/s41580-021-00433-y

Boyman L, Williams GSB, Khananshvili D, Sekler I, Lederer WJ (2013) NCLX: The mitochondrial sodium calcium exchanger. https://doi.org/10.1016/j.yjmcc.2013.03.012

Cox DA, Conforti L, Sperelakis N, Matlib MA (1993) Selectivity of inhibition of Na⁺-Ca²⁺ exchange of heart mitochondria by benzothiazepine CGP-37157. https://doi.org/10.1097/00005344-199304000-00013

de Brito OM, Scorrano L (2008) Mitofusin 2 tethers endoplasmic reticulum to mitochondria. https://doi.org/10.1038/nature07534

Feno S, Rizzuto R, Raffaello A, Vecellio Reane D (2021) The molecular complexity of the mitochondrial calcium uniporter. https://doi.org/10.1016/j.ceca.2020.102322

Fiskum G, Craig SW, Decker GL, Lehninger AL (1980) The cytoskeleton of digitonin-treated rat hepatocytes. https://doi.org/10.1073/pnas.77.6.3430

Fiskum G, Kowaltowski AJ, Andreyev AY, Kushnareva YE, Starkov AA (2000) Apoptosis-related activities measured with isolated mitochondria and digitonin-permeabilized cells. https://doi.org/10.1016/S0076-6879(00)22023-5

Giacomello M, Pyakurel A, Glytsou C, Scorrano L (2020) The cell biology of mitochondrial membrane dynamics. https://doi.org/10.1038/s41580-020-0210-7

Giorgi C, Marchi S, Pinton P (2018) The machineries, regulation and cellular functions of mitochondrial calcium. https://doi.org/10.1038/s41580-018-0052-8

Gnaiger E - MitoEAGLE Task Group (2020) Mitochondrial physiology. https://doi.org/10.26124/bec:2020-0001.v1

Gnaiger E (2020) Mitochondrial pathways and respiratory control. An introduction to OXPHOS analysis. https://doi.org/10.26124/bec:2020-0002

Gostimskaya I, Galkin A (2010) Preparation of highly coupled rat heart mitochondria. https://doi.org/10.3791/2202

Grynkiewicz G, Poenie M, Tsien RY (1985) A new generation of Ca²⁺ indicators with greatly improved fluorescence properties. https://doi.org/10.1016/S0021-9258(19)83641-4

Haworth RA, Hunter DR, Berkoff HA (1980) Na$^+$ releases Ca^{2+} from liver, kidney and lung mitochondria. https://doi.org/10.1016/0014-5793(80)80076-7

Jadiya P, Kolmetzky DW, Tomar D, Di Meco A, Lombardi AA, Lambert JP, Luongo TS, Ludtmann MH, Praticò D, Elrod JW (2019) Impaired mitochondrial calcium efflux contributes to disease progression in models of Alzheimer's disease. https://doi.org/10.1038/s41467-019-11813-6

Kowaltowski AJ, Menezes-Filho SL, Assali EA, Gonçalves IG, Cabral-Costa JV, Abreu P, Miller N, Nolasco P, Laurindo FRM, Bruni-Cardoso A, Shirihai OS (2019) Mitochondrial morphology regulates organellar Ca^{2+} uptake and changes cellular Ca^{2+} homeostasis. https://doi.org/10.1096/fj.201901136R

Kristián T, Weatherby TM, Bates TE, Fiskum G (2002) Heterogeneity of the calcium-induced permeability transition in isolated non-synaptic brain mitochondria. https://doi.org/10.1046/j.1471-4159.2002.01238.x

Kuo IY, Brill AL, Lemos FO, Jiang JY, Falcone JL, Kimmerling EP, Cai Y, Dong K, Kaplan DL, Wallace DP, Hofer AM, Ehrlich BE (2019) Polycystin 2 regulates mitochondrial Ca^{2+} signaling, bioenergetics, and dynamics through mitofusin 2. https://doi.org/10.1126/scisignal.aat7397

Kuznetsov AV, Veksler V, Gellerich FN, Saks V, Margreiter R, Kunz WS (2008) Analysis of mitochondrial function in situ in permeabilized muscle fibers, tissues and cells. https://doi.org/10.1038/nprot.2008.61

Minta A, Kao JPY, Tsien RY (1989) Fluorescent indicators for cytosolic calcium based on rhodamine and fluorescein chromophores. https://doi.org/10.1016/S0021-9258(18)83165-9

Nita II, Hershfinkel M, Fishman D, Ozeri E, Rutter GA, Sensi SL, Khananshvili D, Lewis EC, Sekler I (2012) The mitochondrial Na$^+$/Ca^{2+} exchanger upregulates glucose dependent Ca^{2+} signalling linked to insulin secretion. https://doi.org/10.1371/journal.pone.0046649

Palty R, Silverman WF, Hershfinkel M, Caporale T, Sensi SL, Parnis J, Nolte C, Fishman D, Shoshan-Barmatz V, Herrmann S, Khananshvili D, Sekler I (2010) NCLX is an essential component of mitochondrial Na$^+$/Ca^{2+} exchange. https://doi.org/10.1073/pnas.0908099107

Pathak T, Gueguinou M, Walter V, Delierneux C, Johnson MT, Zhang X, Xin P, Yoast RE, Emrich SM, Yochum GS, Sekler I, Koltun WA, Gill DL, Hempel N, Trebak M (2020) Dichotomous role of the human mitochondrial Na$^+$/Ca^{2+}/Li$^+$ exchanger NCLX in colorectal cancer growth and metastasis. https://doi.org/10.7554/eLife.59686

Rizzuto R, De Stefani D, Raffaello A, Mammucari C (2012) Mitochondria as sensors and regulators of calcium signalling. https://doi.org/10.1038/nrm3412

Rossi A, Pizzo P, Filadi R (2019) Calcium, mitochondria and cell metabolism: A functional triangle in bioenergetics. https://doi.org/10.1016/j.bbamcr.2018.10.016

Rudolf R, Mongillo M, Rizzuto R, Pozzan T (2003) Looking forward to seeing calcium. https://doi.org/10.1038/nrm1153

Rysted JE, Lin Z, Walters GC, Rauckhorst AJ, Noterman M, Liu G, Taylor EB, Strack S, Usachev YM (2021) Distinct properties of Ca^{2+} efflux from brain, heart and liver mitochondria: The effects of Na$^+$, Li$^+$ and the mitochondrial Na$^+$/Ca^{2+} exchange inhibitor CGP37157. https://doi.org/10.1016/j.ceca.2021.102382

Saks VA, Veksler VI, Kuznetsov AV, Kay L, Sikk P, Tiivel T, Tranqui L, Olivares J, Winkler K, Wiedemann F, Kunz WS (1998) Permeabilized cell and skinned fiber techniques in studies of mitochondrial function in vivo. https://doi.org/10.1023/A:1006834912257

Schmidt CA, Kelsey H, Fisher-Wellman, Darrell Neufer P (2021) From OCR and ECAR to energy: Perspectives on the design and interpretation of bioenergetics studies. https://doi.org/10.1016/j.jbc.2021.101140

Serna JDC, Amaral AG, Caldeira da Silva CC, Munhoz AC, Vilas-Boas EA, Menezes-Filho SL, Kowaltowski AJ (2022) Regulation of kidney mitochondrial function by caloric restriction. https://doi.org/10.1152/ajprenal.00461.2021

Serna JDC, Caldeira da Silva CC, Kowaltowski AJ (2020) Functional changes induced by caloric restriction in cardiac and skeletal muscle mitochondria. https://doi.org/10.1007/s10863-020-09838-4

Spinelli JB, Haigis MC (2018) The multifaceted contributions of mitochondria to cellular metabolism. https://doi.org/10.1038/s41556-018-0124-1

Tahara EB, Navarete FD, Kowaltowski AJ (2009) Tissue-, substrate-, and site-specific characteristics of mitochondrial reactive oxygen species generation. https://doi.org/10.1016/j.freeradbiomed.2009.02.008

Vercesi AE, Bernardes CF, Hoffmann ME, Gadelha FR, Docampo R (1991) Digitonin permeabilization does not affect mitochondrial function and allows the determination of the mitochondrial membrane potential of *Trypanosoma cruzi* in situ. https://www.jbc.org/article/S0021-9258(18)98703-X/pdf

Vercesi AE, Castilho RF, Kowaltowski AJ, de Oliveira HCF, de Souza-Pinto NC, Figueira TR, Busanello ENB (2018) Mitochondrial calcium transport and the redox nature of the calcium-induced membrane permeability transition. https://doi.org/10.1016/j.freeradbiomed.2018.08.034

Vilas-Boas EA, Cabral-Costa JV, Ramos VM, da Silva CCC, Kowaltowski AJ (2022) Goldilocks calcium and the mitochondrial respiratory chain: too much, too little, just right. https://doi.org/10.1101/2022.04.12.488015

Whitaker, M (2010) Genetically encoded probes for measurement of intracellular calcium. https://doi.org/10.1016/B978-0-12-374841-6.00006-2

Williams GSB, Boyman L, Chikando AC, Khairallah RJ, Lederer WJ (2013) Mitochondrial calcium uptake. https://doi.org/10.1073/pnas.1300410110

Wingrove DE, Gunter TE (1986) Kinetics of mitochondrial calcium transport. I. Characteristics of the sodium-independent calcium efflux mechanism of liver mitochondria. https://www.jbc.org/article/S0021-9258(18)66846-2/pdf